

## Supplementary Information

### First-principles Thermodynamic Calculations and Experimental Investigation of Sr–Si–N–O System—Synthesis of $\text{Sr}_2\text{Si}_5\text{N}_8:\text{Eu}$ Phosphor

*Yongseon Kim<sup>1</sup>, Jaecheol Kim<sup>2</sup> and Shinhoo Kang<sup>2,\*</sup>*

<sup>1</sup>Department of Materials Science and Engineering,  
Inha University, Incheon, 402-751, Korea

<sup>2</sup>Department of Materials Science and Engineering,  
Seoul National University, Seoul, 151-742, Korea

Author E-mail: [ys.kim@inha.ac.kr](mailto:ys.kim@inha.ac.kr)  
[cheol@snu.ac.kr](mailto:cheol@snu.ac.kr)  
[shinkang@snu.ac.kr](mailto:shinkang@snu.ac.kr)

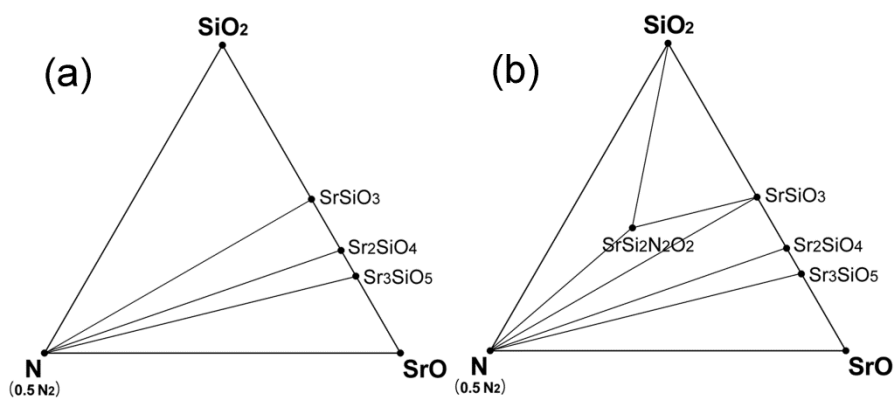
S1. Crystal structure and energy (eV/formula unit) of Sr–Si–N–O system compounds obtained by density functional theory calculation: the energy was used for simulation of phase diagrams.

Compounds	Space group	Energy (eV/fu)	Compounds	Space group	Energy
Sr <sub>5</sub> Si <sub>3</sub>	<i>I 4/mcm</i>	-27.771	S <sub>2</sub> N <sub>2</sub> O	<i>I 4<sub>1</sub>/amd</i>	-39.705
SrSi	<i>Cmcm</i>	-8.096	SiO <sub>2</sub>	<i>P 6<sub>3</sub>/mmc</i>	-23.691
SrSi	<i>Immm</i>	-7.919	SiO <sub>2</sub>	<i>P6<sub>2</sub>22</i>	-23.701
SrSi <sub>2</sub>	<i>I 4<sub>1</sub>/amd</i>	-13.820	SiO <sub>2</sub>	<i>P 3<sub>1</sub>21</i>	-23.704
SrSi <sub>2</sub>	<i>P 4<sub>3</sub>32</i>	-13.579	SrO <sub>2</sub>	<i>I 4/mmm</i>	-17.235
Sr <sub>4</sub> Si <sub>7</sub>	<i>I 4<sub>1</sub>/amd</i>	-48.319	SrO	<i>Fm<math>\bar{3}</math>m</i>	-12.093
Sr <sub>2</sub> Si <sub>3</sub>	<i>I 4<sub>1</sub>/amd</i>	-20.991	SrSiO <sub>3</sub>	<i>P<math>\bar{1}</math></i>	-37.000
SrN	<i>C 2/m</i>	-11.067	SrSiO <sub>3</sub>	<i>P 2<sub>1</sub>/c</i>	-36.913
SrN <sub>2</sub>	<i>I 4/mmm</i>	-19.836	SrSiO <sub>3</sub>	<i>C 2/c</i>	-37.094
Sr <sub>2</sub> N	<i>R<math>\bar{3}</math>m</i>	-13.339	Sr <sub>2</sub> SiO <sub>4</sub>	<i>Pmnb</i>	-49.729
SrN <sub>6</sub>	<i>Fddd</i>	-52.992	Sr <sub>3</sub> SiO	<i>Pbnm</i>	-22.066
Sr <sub>3</sub> N <sub>2</sub>	<i>Ia<math>\bar{3}</math></i>	-24.256	SrN <sub>2</sub> O <sub>6</sub>	<i>Pa<math>\bar{3}</math></i>	-57.976
Si <sub>3</sub> N <sub>4</sub>	<i>I<math>\bar{4}</math>3d</i>	-56.569	SrSi <sub>2</sub> O <sub>5</sub>	<i>Cmca</i>	-59.567
Si <sub>3</sub> N <sub>4</sub>	<i>P 31c</i>	-57.267	SrSi <sub>2</sub> N <sub>2</sub> O <sub>2</sub>	<i>P 1</i>	-52.326
Si <sub>3</sub> N <sub>4</sub>	<i>Fd<math>\bar{3}</math>m</i>	-56.235	Sr <sub>3</sub> SiO <sub>5</sub>	<i>P 4/ncc</i>	-61.837
SrSiN <sub>2</sub>	<i>P 2<sub>1</sub>/c</i>	-28.488	SrSi <sub>6</sub> N <sub>8</sub> O	<i>Imn2</i>	-126.871
SrSi <sub>6</sub> N <sub>8</sub>	<i>Imm2</i>	-117.585			
Sr <sub>2</sub> Si <sub>5</sub> N <sub>8</sub>	<i>Pmn2<sub>1</sub></i>	-114.978	Sr	<i>Fm<math>\bar{3}</math>m</i>	-1.682
SrSi <sub>7</sub> N <sub>10</sub>	<i>Pc</i>	-143.193	Si	<i>Fd<math>\bar{3}</math>m</i>	-5.425

S2. DFT calculation results of energy of Eu-doped compounds: doping amount of Eu, energy of Eu-doped compounds, and energy change of each compound with Eu-doping relative to those of the undoped.

	Eu/(Eu+Sr)	E (eV/fu)	$(E-E_{\text{undoped}})/E_{\text{undoped}}$
SrSi	1/16 (6.25 %)	-8.103	-0.093 %
SrSi <sub>2</sub>	1/16 (6.25 %)	-13.684	+0.983 %
SrSiO <sub>3</sub> (Sr1)	1/12 (8.33 %)	-37.172	-0.212 %
SrSiO <sub>3</sub> (Sr2)	1/12 (8.33 %)	-37.171	-0.208 %
Sr <sub>2</sub> SiO <sub>4</sub> (Sr1)	1/16 (6.25 %)	-49.850	-0.242 %
Sr <sub>2</sub> SiO <sub>4</sub> (Sr2)	1/16 (6.25 %)	-49.873	-0.288 %
SrSiN <sub>2</sub>	1/16 (6.25 %)	-28.545	-0.203 %
SrO	1/32 (3.13 %)	-12.131	-0.312 %
Sr <sub>2</sub> Si <sub>5</sub> N <sub>8</sub> (Sr1)	1/8 (12.5 %)	-115.212	-0.203 %
Sr <sub>2</sub> Si <sub>5</sub> N <sub>8</sub> (Sr2)	1/8 (12.5 %)	-115.208	-0.200 %
SrSi <sub>6</sub> N <sub>8</sub> (Sr1)	1/4 (25.0 %)	-117.732	-0.125 %
SrSi <sub>6</sub> N <sub>8</sub> (Sr2)	1/8 (12.5 %)	-117.657	-0.061 %

S3. Change of phase diagrams with different energy values of  $\text{SrSi}_2\text{N}_2\text{O}_2$ : (a) It is assumed that Sr atoms are not dispersed over different sites but occupies only one type of crystallographic site. This is a simplification for DFT calculation, but it was reported that Sr occupies two sites (with 80:20 ratio). The dispersion may appear because it is energetically more favorable. If we assume actual energy of  $\text{SrSi}_2\text{N}_2\text{O}_2$  is about 92% of the calculated energy and simulate phase diagram using this value,  $\text{SrSi}_2\text{N}_2\text{O}_2$  appeared as a thermodynamic stable phase, as shown in (b). (both of the diagrams are simulated at 1500K under HRN condition.)



S4. Chemical potential of oxygen: the 0 K chemical potential was determined from combination of formation enthalpies of various metal oxides and DFT-calculated energies, as discussed in the manuscript. The effects of temperature and pressure were reflected based on the data in JANAF thermochemical tables using the following equation:

$$\mu_{\text{O}_2}(T,P) = H^{\circ}(T) - TS^{\circ}(T) + k_{\text{B}}T \ln \frac{P}{P^{\circ}}$$

We present chemical potential of oxygen at  $p_{\text{O}_2} = 0.1$  MPa and 0.02MPa in the following table as an example.

T (K)	$\mu_{\text{O}_2}$ (eV)	
	$p_{\text{O}_2} = 0.1$ MPa	$p_{\text{O}_2} = 0.02$ MPa
0	-8.450	-8.450
100	-8.585	-8.599
200	-8.763	-8.790
298	-8.952	-8.993
300	-8.956	-8.997
400	-9.158	-9.214
500	-9.368	-9.437
600	-9.583	-9.666
700	-9.803	-9.900
800	-10.028	-10.138
900	-10.256	-10.381
1000	-10.488	-10.627
1100	-10.724	-10.877
1200	-10.963	-11.130
1300	-11.205	-11.386
1400	-11.450	-11.644
1500	-11.698	-11.906
1600	-11.948	-12.170
1700	-12.200	-12.436
1800	-12.455	-12.704
1900	-12.711	-12.975
2000	-12.970	-13.247

S5. Chemical potential of nitrogen gas, which is calculated in the same manner with that of oxygen shown in S4.

T (K)	$\mu_{\text{N}_2}$ (eV)	
	$p_{\text{N}_2} = 0.1$ MPa	$p_{\text{N}_2} = 0.08$ MPa
0	-16.050	-16.050
100	-16.186	-16.187
200	-16.363	-16.366
298	-16.552	-16.557
300	-16.556	-16.561
400	-16.759	-16.767
500	-16.970	-16.979
600	-17.187	-17.198
700	-17.409	-17.422
800	-17.636	-17.651
900	-17.867	-17.884
1000	-18.101	-18.121
1100	-18.340	-18.361
1200	-18.581	-18.604
1300	-18.825	-18.850
1400	-19.072	-19.098
1500	-19.321	-19.350
1600	-19.573	-19.603
1700	-19.827	-19.859
1800	-20.083	-20.117
1900	-20.341	-20.378
2000	-20.601	-20.640